scientific reports

Check for updates

OPEN

Numerical simulation of bioconvective Darcy Forchhemier nanofluid flow with energy transition over a permeable vertical plate

Ebrahem A. Algehyne[1,2], Mounirah Areshi[1], Anwar Saeed[3], Muhammad Bilal[4], Wiyada Kumam[5] & Poom Kumam[3,6]✉

In biological systems, the MHD boundary layer bioconvection flow through permeable surface has several applications, including electronic gadgets, heating systems, building thermal insulation, geological systems, renewable energy, electromagnetism and nuclear waste. The bioconvection caused by the hydromagnetic flow of a special form of water-based nanoliquid including motile microorganisms and nanoparticles across a porous upright moving surface is investigated in this report. The combination of motile microbes and nanoparticles causes nanofluid bioconvection is studied under the cumulative impact of magnetic fields and buoyancy forces. The Brownian motion, thermophoresis effects, heat absorption/generation, chemical reaction and Darcy Forchhemier impact are also unified into the nonlinear model of differential equations. The modeled boundary value problem is numerically computed by employing a suitable similarity operation and the parametric continuation procedure. The parametric study of the flow physical parameters is evaluated versus the velocity, energy, volume fraction of nanoparticles, motile microorganisms' density, skin friction, Sherwood number and Nusselt number. It has been observed that the velocity profile reduces with the effect of porosity parameter k_1, inertial parameter k_2, Hartmann number and buoyancy ratio. While the energy transition profile significantly enhances with the flourishing values of Eckert number *Ec*, heat absorption/generation *Q* and Hartmann number respectively.

List of symbols

B_0	Applied magnetic field
(u, v)	Velocity component
Q_0	Heat generation/absorption
$k = k_0 x$	Initial permeability
g	Gravity
σ	Electrical conductivity
$f_w < 0$	Injection
Wc	Cell moving speed
n	Concentration of the microorganisms

[1]Department of Mathematics, Faculty of Science, University of Tabuk, P.O. Box 741, Tabuk 71491, Saudi Arabia. [2]Nanotechnology Research Unit (NRU), University of Tabuk, Tabuk 71491, Saudi Arabia. [3]Center of Excellence in Theoretical and Computational Science (TaCS-CoE), Faculty of Science, King Mongkut's University of Technology Thonburi (KMUTT), 126 Pracha Uthit Rd., Bang Mod, Thung Khru, Bangkok 10140, Thailand. [4]Department of Mathematics, City University of Science and Information Technology, Peshawar 25000, Pakistan. [5]Applied Mathematics for Science and Engineering Research Unit (AMSERU), Program in Applied Statistics, Department of Mathematics and Computer Science, Faculty of Science and Technology, Rajamangala University of Technology Thanyaburi, Thanyaburi, Pathumthani 12110, Thailand. [6]Department of Medical Research, China Medical University Hospital, China Medical University, Taichung 40402, Taiwan. ✉email: poom.kum@kmutt.ac.th

n_w	Density of motile microbes
T_w	Surface temperature
$f_w = 0$	Surface impermeability
Gr	Grashof number
Pe	Péclet number
Lb	Bioconvection Lewis number
Ha	Hartmann number
Nb	Brownian motion
λ	Ratio of the heat capacitance to the base fluid
ρ_f	Density
D_B	Brownian diffusion
α	Thermal diffusivity
D_m	Microorganism's diffusivity
β	Volume expansion
μ	Viscosity
γ	Microorganism average volume
b	Chemotaxis coefficient
ρ_m	Density of microorganisms.
ϕ_w	Volume fraction of nanoparticle
$a > 0$	Stretching rate
$f_w > 0$	Suction
Rb	Rayleigh number
Ec	Eckert number
Le	Lewis number
Nt	Thermophoresis constraint
Nr	Buoyancy ratio
Ω	Microorganisms' concentration difference

Boundary layer flow across a porous media has numerous implementations in chemical, civil and mechanical engineering, including electronic gadget cooling, heating system, renewable energy, building thermal insulation, geological systems, non-Newtonian biochemical mechanisms, electromagnetism, and underground treatment of waste of atomic or non-nuclear waste, among many others. Thermal transmission augmentation is of current interest in all of these systems from an energy-saving standpoint. Heat transfer may be improved in a variety of methods, including modifying flow shape, boundary conditions, or increasing the fluid's thermal conductivity. Various theoretical and practical research has revealed that suspending greater thermal conductivity micro solid particles improves base fluid heat transfer properties. However, micro-channels erosion and logging arise due to the enormous size of the colloidal materials. As with nanofluids, the use of relatively smaller particulate (nanoparticles) is recommended as a solution to this problem[1–6]. Noghrehabadi et al.[7] addressed the energy transport and entropy production of a nanoliquid over an adiabatic linear shrinking sheet with energy generation. Increases in heat production occur with the upshot of Brownian motion in the region of the sheet, according to the findings. Khan et al.[8,9] reported the rheological effects of Eyring Powell NF as well as the swimming features of gyrotactic microbes on the surface of a porous medium-encased Riga plate. Reza-E-Rabbi et al.[10,11] and Al-Mamun et al.[12] addressed the hydrodynamic flow characteristics of multiphase radiative Maxwell and Casson fluids across a stretched surface containing nano-sized particles. Bhatti et al.[13] considered the nanoliquid flow with the energy propagating across a Riga plate. The microorganisms and nanofluids saturated in the base fluid are poured into the Riga plate. The results demonstrate that the Rayleigh number and magnetic field of bioconvection diminish the velocity field. Zhang et al.[14] used PCM to investigate the momentum and energy transfer formed by a wavy fluctuation of the surface. Algehyne et al.[15] demonstrated characteristics of MHD Prandtl nanofluid flow on an extended sheet while considering convective boundary conditions. Khan et al.[16–18] demonstrated a 2D flow of bioconvective Eyring–Powell NFs on a upright plate. AlQdah et al.[19] used the bvp4c method to provide a numerical model of dusty NF flow. To emphasize the influence of physical characteristics on mass and heat transmission, qualitative and quantitative explanations are presented. The mixing effect can greatly boost the thermal conductivity of NFs, according to the propagation data.

The study of fluid flow under the consequences of magnetohydrodynamic (MHD) has a huge implementation in the field of geophysics[20], earthquakes[21], astrophysics, sensors, engineering and magnetic drug targeting[22]. Due to its applicability in the biological field, MHD fluid flow in various geometries, rather than industrial applications, relevant to human body parts, is a fascinating and vital scientific subject. Simple flow, pulsatile flow, peristaltic flow, and drug transport are some of the biological applications of MHD[23]. Bilal et al.[24] assessed the convective flow of the hybrid ferrofluid under the principle of electromagnetic induction. Zhou et al.[25] evaluated the MHD Maxwell nanoliquids flow over a porous whirling disc. The energy transmission appears to increase dramatically as the thermophoresis parameter is amplified. Shuaib et al.[26] depicted a 3D nanoliquid communication across two simultaneous spinning plates using hydrodynamics. Their goal was to investigate the cumulative impact of magnetic and electric fields on fluid flow with heat conduction properties. Goyal et al.[27] inspected the issue of threefold diffusive flow having magnetic flux interaction toward a power-law extending sheet using Galerkin finite-element computation. The insights of that study enable industrial corporations in achieving the required product quality by allowing them to manage the frequency of heat transmission. Ghasemi & Hatami[28] examined the properties of solar radiation on 3D nanoliquid flow across a stretched sheet. The magnetic arena was taken into account, and the nonlinear Rosseland approximation is used to calculate heat

radiation. Rasool et al.[29] used the Darcy-Forchheimer correlation to study the temperature communication trends in Jeffery ferrofluid flow across a stretched surface. The electro-magnetic conductivity of the nanoliquid is reinforced by a changing magnetic effect. Small magnetic Reynolds, on the other hand, is thought to negate the generated magnetic effect. Mabood et al.[30] deliberate the characterization of unstable 2D hybrid nanoliquid flow on a smooth strained superficial with the analysis of thermal and MHD effect. The temperature distribution caused by its upward and downstream movement of a flexible spinning disc has been examined by Shuaib et al.[31,32], under the significance of the magnetic field. The MHD hybrid nanofluid flow over different geometries with the bioconvection has been reported by[33–37].

In biotechnology and biological systems, bioconvection has several applications. The idea of nanofluid bioconvection, which is the subject of the research, illustrates how the simultaneous interplay of denser self-propelled microorganisms, buoyancy forces, and nanoparticles causes spontaneous pattern development and density stratification. Gravitaxis, oxytaxis and gyrotaxis organisms are examples of these microbes. Microscale mixing, Increased mass transfer, especially in micro volumes, and improved NF stability are all advantages of motile microorganisms' suspension[38]. The oxytactic microorganisms induce hydrodynamic convection, which creates a flow system that transports cells and oxygen from the higher to lower fluid areas. The nanoparticles are not self-driven, and their flow is administered by Brownian motion. As a result, the mobility of motile bacteria appears to be autonomous of the gesture of nanomaterials[39]. The subject of gyrotactic microorganism bioconvection in nanofluids was initially addressed in[39–41]. Kuznetsov[42] expanded the theory of suspensions by using Buongiorno's conception of bioconvection in nanofluids, which included Brownian motion and thermophoresis. Xu et al.[43] researched an incompressible, stable nanoliquid made up of gyrotactic microorganisms that flowed between parallel surfaces and transferred energy. When the buoyancy convection parameters rise, the velocity profile exhibits a positive reaction. Waqas et al.[44] & Ramzan et al.[45] evaluated the ion and Hall slip in a 3D electrically conducting bioconvective NF flow across a stretched sheet under the influence of a magnetic field. Even though the above-mentioned studies have already been concerned with recognizing nanofluid bioconvection, there has been no endeavor in the literature to explore the consequences of Darcy Forchhemier, heat absorption/generation, magnetic field and chemical reaction on nanofluid bioconvection. For biomedical and industrial applications, such a study may provide some visibility into the complicated dynamics of self-propelled microbes in nanoliquid under the presence of external magnetism[46–48].

The goal of this research is to expand on Olanrewaju and Makinde's work[49–51] by including hydromagnetic nanofluid and Darcy and heat absorption/generation effect on bioconvection across a vertical permeable plate. Because motile microbes are self-driven, they may swim aggressively in the fluid. Nanoparticles, on the other hand, travel owing to Brownian motion and are transported by the fluid flow. The model is expressed, analyzed, and numerically solved in the parts that follow. The most important findings are graphed and explained.

Mathematical formulation. The boundary layer gyrostatic microorganisms conducting flow water-based nanoliquid across a vertical permeable plate is addressed in the present work. A constant transversal magnetic field of intensity B_0 is applied to the flow as shown in Fig. 1. The Hall effects and magnetic field are inconsequential since there is no magnetic Reynolds number and voltage is modest. As stated, the presence of nanoparticles is expected to not influence the velocity and direction of microorganisms' movement. The nanoparticulate dispersion is considered to be steady (no nanoparticle coagulation) and dilute (no particulate concentration more than 1%). This is a reasonable postulation because nanoliquid bioconvection is only predicted to occur in a diluted suspension of nanomaterials; otherwise, a high concentration of nanomaterials would raise the base fluid's viscosity, suppressing bioconvection. The framework for bioconvection due to oxytactic microbes is premised on the methodology described in[49–51]. The modeled equations are expressed as:

$$\frac{\partial u}{\partial x}+\frac{\partial v}{\partial y}=0, \tag{1}$$

$$\begin{aligned} u\frac{\partial u}{\partial x}+v\frac{\partial u}{\partial y}=&-\frac{1}{\rho_f}\frac{\partial p}{\partial x}+\nu_f\frac{\partial^2 u}{\partial y^2}-\frac{\sigma B_0^2 u}{\rho_f}+\frac{1}{\rho_f}\begin{bmatrix}(1-\phi_\infty)\rho_f(T-T_\infty)\beta g-\left(\rho_p-\rho_f\right)\\(\phi-\phi_\infty)g-(n-n_\infty)\left(\rho_m-\rho_f\right)g\gamma\end{bmatrix}\\&-\frac{\nu}{k}(u-U_\infty)-\frac{k'}{\sqrt{k}}(u^2-U_\infty^2),\end{aligned} \tag{2}$$

$$u\frac{\partial T}{\partial x}+v\frac{\partial T}{\partial y}=\alpha\left(\frac{\partial^2 T}{\partial x^2}+\frac{\partial^2 T}{\partial y^2}\right)+\lambda\left\{\begin{matrix}D_B\frac{\partial\phi}{\partial y}\frac{\partial T}{\partial y}+\left(\frac{D_T}{T_\infty}\right)\\\left[\left(\frac{\partial T}{\partial x}\right)^2+\left(\frac{\partial T}{\partial y}\right)^2\right]\end{matrix}\right\}+\frac{\mu\alpha}{k}\left(\frac{\partial u}{\partial y}\right)^2+\frac{\alpha\sigma B_0^2u^2}{k}+\frac{Q_0}{(\rho c)_f}(T-T_\infty), \tag{3}$$

$$u\frac{\partial\phi}{\partial x}+v\frac{\partial\phi}{\partial y}=D_B\left(\frac{\partial^2\phi}{\partial x^2}+\frac{\partial^2\phi}{\partial y^2}\right)+\left(\frac{\partial^2 T}{\partial x^2}+\frac{\partial^2 T}{\partial y^2}\right)\left(\frac{D_T}{T_\infty}\right)-k(\phi-\phi_0), \tag{4}$$

$$u\frac{\partial n}{\partial x}+v\frac{\partial n}{\partial y}+\frac{bW_c}{(\phi_w-\phi_\infty)}\left[\frac{\partial}{\partial y}\left(n\frac{\partial\phi}{\partial y}\right)+\frac{\partial}{\partial x}\left(n\frac{\partial\phi}{\partial x}\right)\right]=D_m\left(\frac{\partial^2 n}{\partial x^2}+\frac{\partial^2 n}{\partial y^2}+2\frac{\partial^2 n}{\partial x\partial y}\right). \tag{5}$$

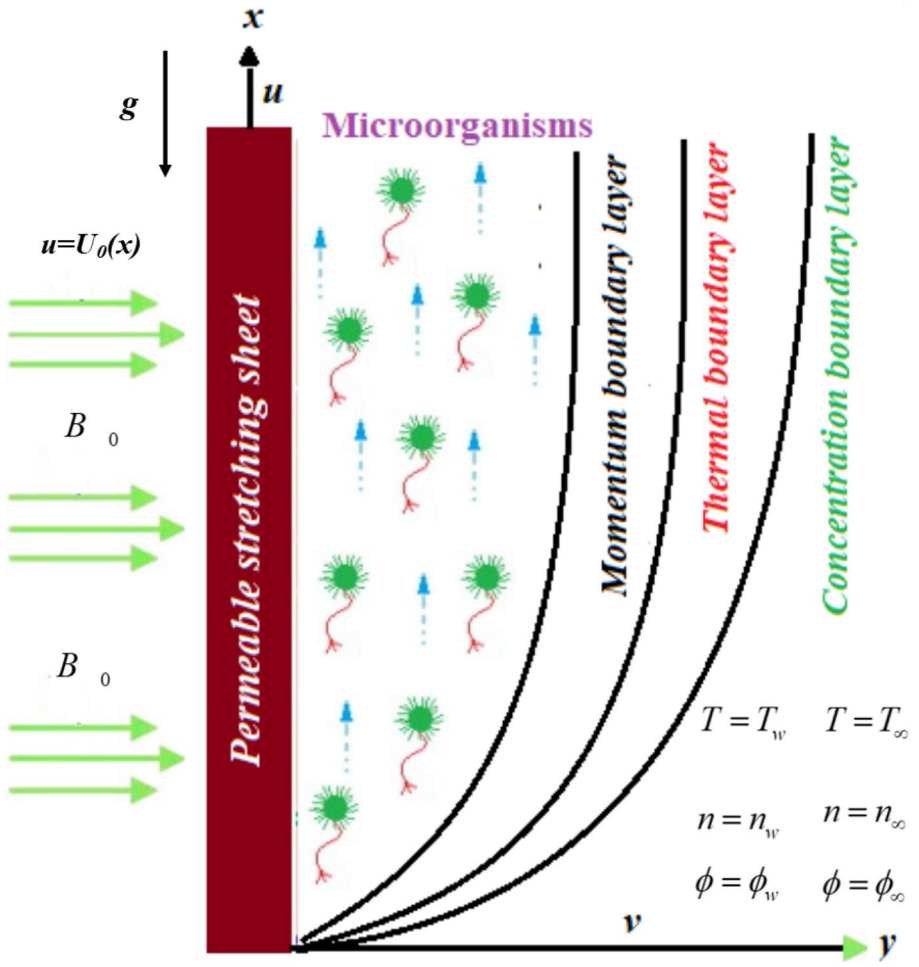

Figure 1. Fluid flow through vertical permeable plate.

Here (u, v) determine the velocity component, ρ_f is the density, Q_0 is the heat source, U_∞ is the uniform free stream velocity, α is the thermal diffusivity, $k = k_0 x$ is the Darcy permeability of the permeable medium, $k' = \frac{k_0}{\sqrt{x}}$ is the Forchhemier resistance,k_0 is the initial permeability, D_m is the microorganisms diffusivity, g and β are the gravity and volume expansion, σ is the electrical conductivity, μ is the viscosity, $\lambda = (\rho C)_p(\rho C)_f$ is the ratio of the heat capacitance to the base fluid, γ is the microorganism average volume, Wc is cell moving speed, b is the chemotaxis coefficient, n is the concentration of the microorganisms and ρ_m represent their density.

The boundary conditions are:

$$\begin{aligned} &u = U_0(x), \quad v = V, \quad T = T_w, \quad \phi = \phi_w, \quad n = n_w \quad \text{at} \quad y = 0, \\ &u = 0, \quad v = 0, \quad T \to T_\infty, \quad \phi \to \phi_\infty, \quad n \to n_w \quad \text{as} \quad y \to \infty. \end{aligned} \tag{6}$$

where n_w, ϕ_w, T_w are the density of motile microbes, volume fraction of nanoparticle and surface temperature. Similarly, the ambient values are signified as $n_\infty, \phi_\infty, T_\infty$ respectively.

The suction/injection velocity and free stream velocity are presumed as[50]:

$$U_0(x) = a\,x \quad \text{and} \quad V = -(a\,v)^{1/2} f_w. \tag{7}$$

Here, $a > 0$ is the stretching rate of the plate, $f_w = 0$ displays the surface impermeability, $f_w > 0$ characterizes suction, and $f_w < 0$ represents injection case.

Presenting the subsequent dimensionless variables:

$$\eta = y(a/v)^{1/2}, \quad \psi = y(av)^{1/2} x f(\eta), \quad \theta(\eta) = \frac{T - T_\infty}{T_f - T_\infty}, \quad \zeta(\eta) = \frac{\varphi - \varphi_\infty}{\varphi_f - \varphi_\infty}, \quad \chi(\eta) = \frac{n - n_\infty}{n_f - n_\infty}. \tag{8}$$

We get

$$f''' + ff'' - (k_2 + 1)\left(f'\right)^2 + Gr(\theta - \zeta Nr - \chi Rb) - Haf' - k_1 f' = 0, \tag{9}$$

$$\theta'' + \theta'\left(Prf + Nb\zeta'\right) + Nt\left(\theta'\right)^2 + Ec\,Pr\left(\left(f''\right)^2 + \left(f'\right)^2 Ha\right) + Q\theta = 0, \tag{10}$$

$$\zeta'' + Lef\zeta' + \frac{Nt}{Nb}\theta'' - d_1\zeta = 0, \tag{11}$$

$$\chi'' + Lbf\chi' - Pe\left[\zeta''(\chi + \Omega) + \zeta'\chi'\right] = 0. \tag{12}$$

Here, $\Omega = \frac{n_\infty}{n_w - n_\infty}$ is the microorganisms concentration difference, $Gr = \frac{\beta\rho_f(1-\phi_\infty)(T_w - T_\infty)}{aU_0}$ is the Grashof number, $Rb = \frac{\gamma(n_w - n_\infty)(\rho_m - \rho_f)}{\beta\rho_f(1-\phi_\infty)(T_w - T_\infty)}$ is the Rayleigh number, $Pe = \frac{bW_c}{D_m}$ is the bioconvection Péclet number, $Ec = \frac{U_0^2}{C_{pf}(T_f - T_\infty)}$ is the Eckert number, $Lb = \frac{\nu}{D_m}$ is the bioconvection Lewis number, $Le\frac{\nu}{D_B}$ is the Lewis number, $Pr = \frac{\nu}{\alpha}$ is the Prandtl number, $Ha = \frac{\sigma B_0^2}{a\rho_f}$ is the Hartmann number, $Nt = \frac{\lambda D_T(T_w - T_\infty)}{\alpha}$ is the thermophoresis constraint, $Nb = \frac{\lambda D_B(\varphi_w - \varphi_\infty)}{\alpha}$ is the Brownian motion, $Nr = \frac{(\rho_f - \rho_{f\infty})(\varphi_w - \varphi_\infty)}{\beta\rho_f(1-\varphi_\infty)(T_w - T_\infty)}$ is the buoyancy ratio,

The transform conditions are:

$$\left.\begin{aligned} &f'(0) = 1, \quad f(0) = f_w, \quad \zeta(0) = 1, \quad \theta(0) = 1, \quad \chi(0) = 1,\\ &f'(\infty) = 0, \quad \zeta(\infty) = 0, \quad \theta(\infty) = 0, \quad \chi(\infty) = 0. \end{aligned}\right\} \tag{13}$$

The practical interest quantities of this study are[50]:

$$C_f = \frac{\tau_w}{\rho_f u_0^2}, \quad Nu = \frac{xq_w}{k_f\left(T_f - T_\infty\right)}, \quad Sh = \frac{xq_m}{D_B(\phi_w - \phi_\infty)}, \quad Nn = \frac{xq_n}{(n_w - n_\infty)D_n}. \tag{14}$$

where $\tau_w,\ q_w,\ q_m,\ q_n$ are the skin friction, energy flux, mass flux and motile microorganisms flux defined as:

$$\tau_w = \mu\left(\frac{\partial u}{\partial y}|_{y=o}\right),\ q_w = -k\left(\frac{\partial T}{\partial y}|_{y=o}\right),\ q_m = -D_B\left(\frac{\partial \zeta}{\partial y}|_{y=o}\right),\ q_n = -Dn\left(\frac{\partial \chi}{\partial y}|_{y=o}\right). \tag{15}$$

From (14) & (15), we get:

$$\left.\begin{aligned} &C_{fx} = Re_x^{1/2}C_f = f''(0), \quad Nu_x = Re_x^{-1/2}Nu = -\theta'(0),\\ &Sh_x = Re_x^{-1/2}Sh = -\zeta'(0), \quad Nn_x = Re_x^{-1/2}Nn = -\chi'(0). \end{aligned}\right\} \tag{16}$$

Numerical solution. PCM frequently solved the complicated nonlinear boundary value problems that are typically handled by other numerical techniques[52,53]. The subsequent stages demonstrate the essential concept of concerning the PCM approach to a system of ODEs (9–12) & (13).

Step 1: Reducing the BVP to a first-order system ODEs

$$h_1 = f,\ h_2 = f',\ h_3 = f'',\ h_4 = \theta,\ h_5 = \theta',\ h_6 = \zeta,\ h_7 = \zeta',\ h_8 = \chi,\ h_9 = \chi'.$$

Equations (9–12) are reduced as:

$$\left.\begin{aligned} h_3' &= -h_1h_3 + (k_2+1)h_2^2 + Hah_2 - Gr(h_4 - Nrh_6 - Rbh_8) - k_1h_2,\\ h_5' &= -h_5(Pr\,h_1 - Nbh_7) - Nth_5^2 - Pr\,Ec\left(Hah_2^2\right) + Qh_4,\\ h_7' &= -Leh_1h_7d_1 - \frac{Nt}{Nb}\left(-h_5(Pr\,h_1 + Nbh_7) - Nth_5^2 - Pr\,Ec\left(Hah_2^2\right) + Qh_4\right),\\ h_9' &= -Lbh_1h_9 + Pe\left\{(h_8 + \Omega)\left[-Leh_1h_7 - \frac{Nt}{Nb}\left[\begin{matrix} Pr\,h_1h_5 - Nbh_7h_5 - Nth_5^2\\ -Pr\,Ec\left(h_3^2 + Hah_2^2\right) + Qh_4 \end{matrix}\right]\right] + h_7h_9\right\} \end{aligned}\right\} \tag{17}$$

with the boundary conditions.

$$\left.\begin{aligned} &h_1(0) = f_w, \quad h_2(0) = 1, \quad h_3(0) = s_1, \quad h_4(0) = 1, \quad h_5(0) = s_2,\\ &h_6(0) = 1, \quad h_7(0) = s_3, \quad h_8(0) = 1, \quad h_9(0) = s_4. \end{aligned}\right\} \tag{18}$$

Step 2: Introducing parameter p

$$\left.\begin{aligned} h_3' &= -h_1(h_3 - 1)p + (k_2+1)h_2^2 + Hah_2 - Gr(h_4 - Nrh_6 - Rbh_8) - k_1h_2,\\ h_5' &= -(h_5 - 1)p(Pr\,h_1 - Nbh_7) - Nth_5^2 - Pr\,Ec\left(Hah_2^2\right) + Qh_4,\\ h_7' &= -Leh_1(h_7 - 1)pd_1 - \frac{Nt}{Nb}\left(-h_5(Pr\,h_1 + Nbh_7) - Nth_5^2 - Pr\,Ec\left(Hah_2^2\right) + Qh_4\right),\\ h_9' &= -Lbh_1(h_9 - 1)p + Pe\left\{(h_8 + \Omega)\left[-Leh_1h_7 - \frac{Nt}{Nb}\left[\begin{matrix} Pr\,h_1h_5 - Nbh_7h_5 - Nth_5^2\\ -Pr\,Ec\left(h_3^2 + Hah_2^2\right) + Qh_4 \end{matrix}\right]\right] + h_7h_9\right\} \end{aligned}\right\} \tag{19}$$

Step 3: Differentiating by parameter 'p'

Furthermore, by employing the implicit scheme, Eq. (19) has been discretized and computed through PCM. The results are shown and discussed in the next section.

Results and discussion

The discussion segment evaluated the conduct of velocity, energy, nanoparticles concentration and motile microorganism profile as compared to numerous physical. Their out-turns are revealed through the following subsection. While keeping the parameters values are, $k_1 = 0.1, k_2 = 0.1,\ \Omega = 0.1,\ \ Gr = 2.0,\ \ Rb = 0.5,\ \ Pe = 0.3,$ $Ec = 0.1,\ Lb = 0.4,\ Le = 0.1,\ Ha = 1.5,\ Nt = Nb = Nr = 0.3.$

Velocity profile. Figure 2a–f evaluate the nature of velocity $f'(\eta)$ profile versus Hartmann number *Ha,* buoyancy ratio *Nr*, porosity parameter k_1, inertial parameter k_2, bioconvection Rayleigh number *Rb* and Grashof number *Gr* respectively. Figure 2a, b show that the fluid velocity condenses with the effect of Hartmann number and buoyancy ratio. The rising values of Hartmann number *Ha* produce the magnetic effect, where the Lorentz force is fashioned due to magnetic field and that resistive force opposes the fluid flow. The buoyancy effect pushes the fluid towards the sheet edge, reducing both the fluid velocity $f'(\eta)$ and thickness of the momentum boundary layer as publicized in Fig. 2b. Figure 2c, d discovered that the fluid velocity decreases with the upshot of porosity parameter k_1 and inertial constraint k_2. Physically, the porosity effect also produces confrontation to the fluid flow, which results in deacceleration of the velocity field. Figure 2e, f reported that the fluid velocity diminishes with the consequences of bioconvection Rayleigh number and improves with the Grashof number. Both the number have an inverse behavior to each other, that's why their impact also revealed an opposite trend on the velocity distribution $f'(\eta)$.

Energy distribution profile. Figure 3a–e illustrated the conduct of energy transition $\theta(\eta)$ profile versus Eckert number *Ec*, heat absorption/generation *Q*, Hartmann number *Ha*, suction/injection f_w and Brownian motion Nb respectively. Figure 3a–c displayed that the energy transition profile significantly enhances with the flourishing values of Eckert number *Ec*, heat absorption/generation *Q* and Hartmann number respectively. The Eckert number reduces the specific heat capacity and heat driving force, which become the reason for temperature enhancement. Similarly, the heat absorption/generation and Hartmann number effect generate extra heat, which causes escalations in the fluid temperature $\theta(\eta)$. Figure 3d, e manifested that the energy profile diminishes with the rising credit of suction/injection and Brownian motion. During the fluid flow, when suction and injection occurred, the heated particles start evaporating through walls and as a result, the remaining fluid temperature reduces as presented in Fig. 3d.

Nanoparticles concentration profile. Figure 4a–d highlighted the nature of nanoparticles concentration $\varphi(\eta)$ profile versus chemical reaction d_1, thermophoresis constant *Nt*, Lewis number *Le* and Brownian motion *Nb* respectively. Figure 4a, b revealed that the nanoparticles concentration boosts with the effect of chemical reaction d_1 and thermophoresis constant. The variation in chemical reaction accelerates the fluid particles' kinetic energy, which encourages the nanoparticulate profile as spotted in Fig. 4a. On the other hand, the nanoparticles concentration profile significantly decreases with the action of Lewis number. Since the molecular dispersal condenses and kinetic viscosity of fluid upsurges with the Lewis number effect, such a situation has been pragmatic in Fig. 4c, d.

Motile microorganism profile. Figure 5a–d revealed the nature of motile microorganism $\chi(\eta)$ profile versus parameters f_w, *Lb*, Ω and *Pe* respectively. Figure 5a–d highlighted that the motile micro-organism profile effectively diminishes with the rising credit of suction/injection, bioconvection Lewis number, microorganism concentration difference and bio-convection Peclet number respectively.

Table 1 displayed the comparative calculations of the current results with the published work.

Conclusion

The bio-convection caused by the hydromagnetic flow of a special form of water-based nanoliquid including motile microorganisms and nanoparticles across a porous upright moving surface is investigated. The Brownian motion, thermophoresis effects, heat absorption/generation, chemical reaction and Darcy Forchhemier impact are also unified into the nonlinear model of differential equations. The modeled equations are solved computationally by employing suitable similarity operations and the Parametric continuation Procedure. The following observation has been noticed:

- The velocity profile reduces with the upshot of porosity constraint k_1, inertial parameter k_2, Hartmann number and buoyancy ratio.
- The energy transition profile significantly enhances with the flourishing values of Eckert number *Ec*, heat absorption/generation *Q* and Hartmann number respectively.
- The fluid velocity diminishes with the consequences of bioconvection Rayleigh number and improves with the Grashof number. Both the number has an inverse behavior to each other, that's why their impact also revealed an opposite trend on the velocity distribution $f'(\eta)$.
- The rising credit of suction/injection, Brownian motion and Prandtl number decrease the energy profile.

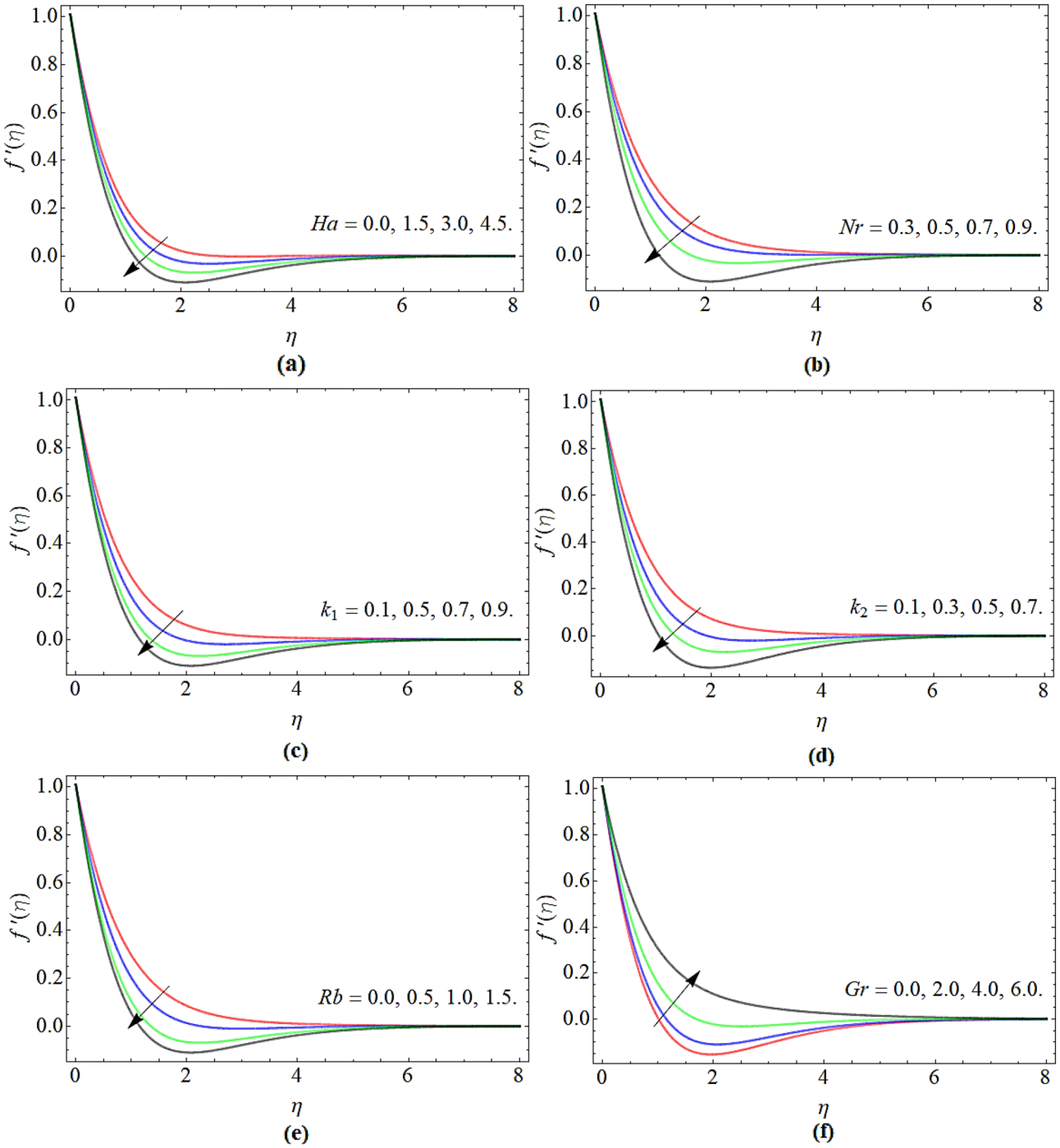

Figure 2. The nature of velocity $f'(\eta)$ profile as opposed to (**a**) Hartmann number *Ha*, (**b**) buoyancy ratio *Nr*, (**c**) porosity parameter k_1, (**d**) inertial parameter k_2, (**e**) bioconvection Rayleigh number *Rb* and (**f**) Grashof number *Gr* respectively.

- The motile micro-organism profile effectively reduces with the intensifying credit of f_w, Lb, Ω, *Pe*.
- The nanoparticles concentration profile boosts with the effect of chemical reaction d_1 and thermophoresis constant, while diminishes with the action of Lewis number *Le* and Brownian motion.

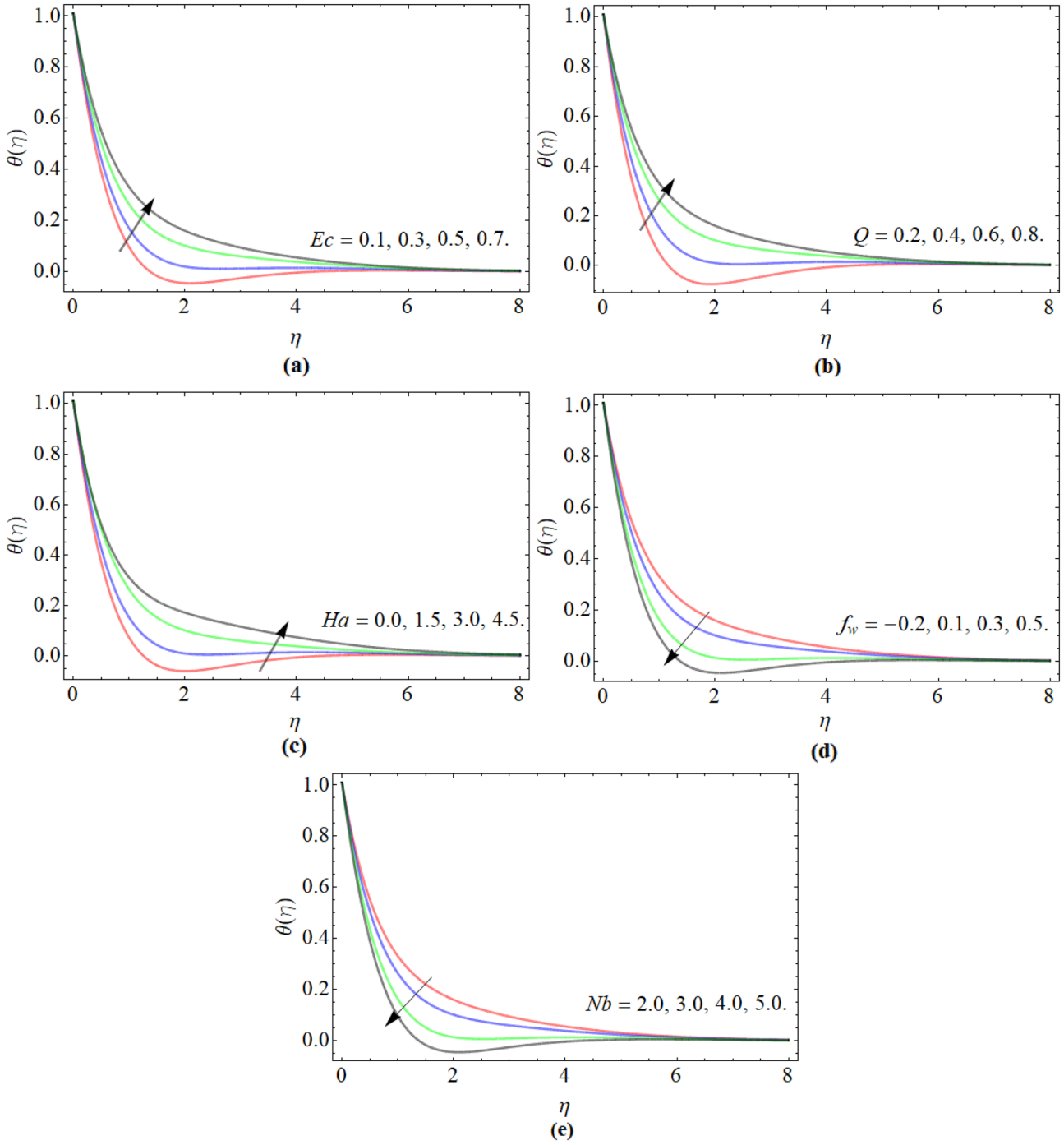

Figure 3. The nature of energy transition $\theta(\eta)$ profile versus (**a**) Eckert number *Ec*, (**b**) heat absorption/generation *Q*, (**c**) Hartmann number *Ha*, (**d**) suction/injection f_w, (**e**) Brownian motion Nb respectively.

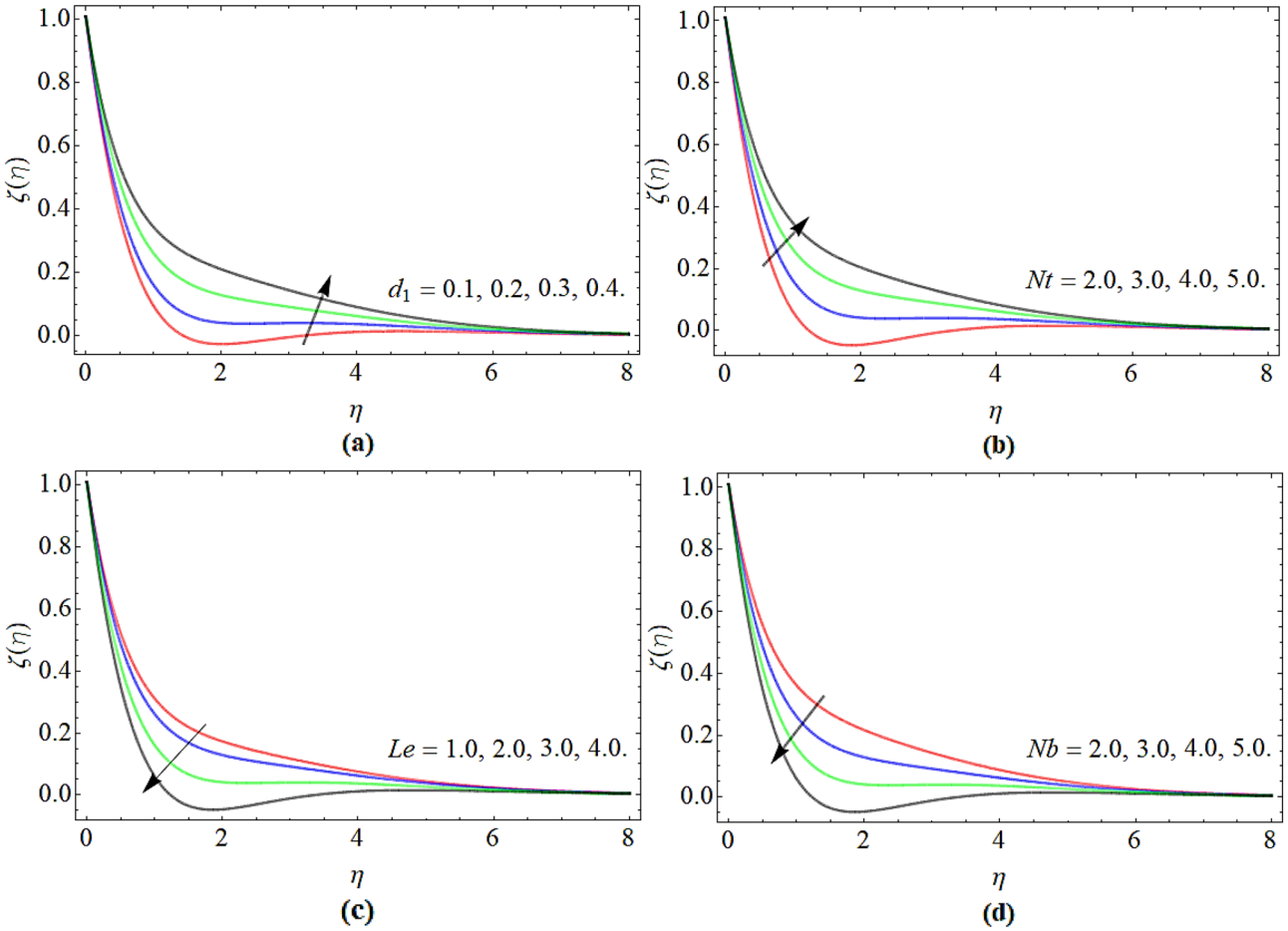

Figure 4. The nature of nanoparticles concentration $\varphi(\eta)$ profile versus (**a**) chemical reaction d_1, (**b**) thermophoresis constant *Nt*, (**c**) Lewis number *Le*, (**d**) Brownian motion *Nb* respectively.

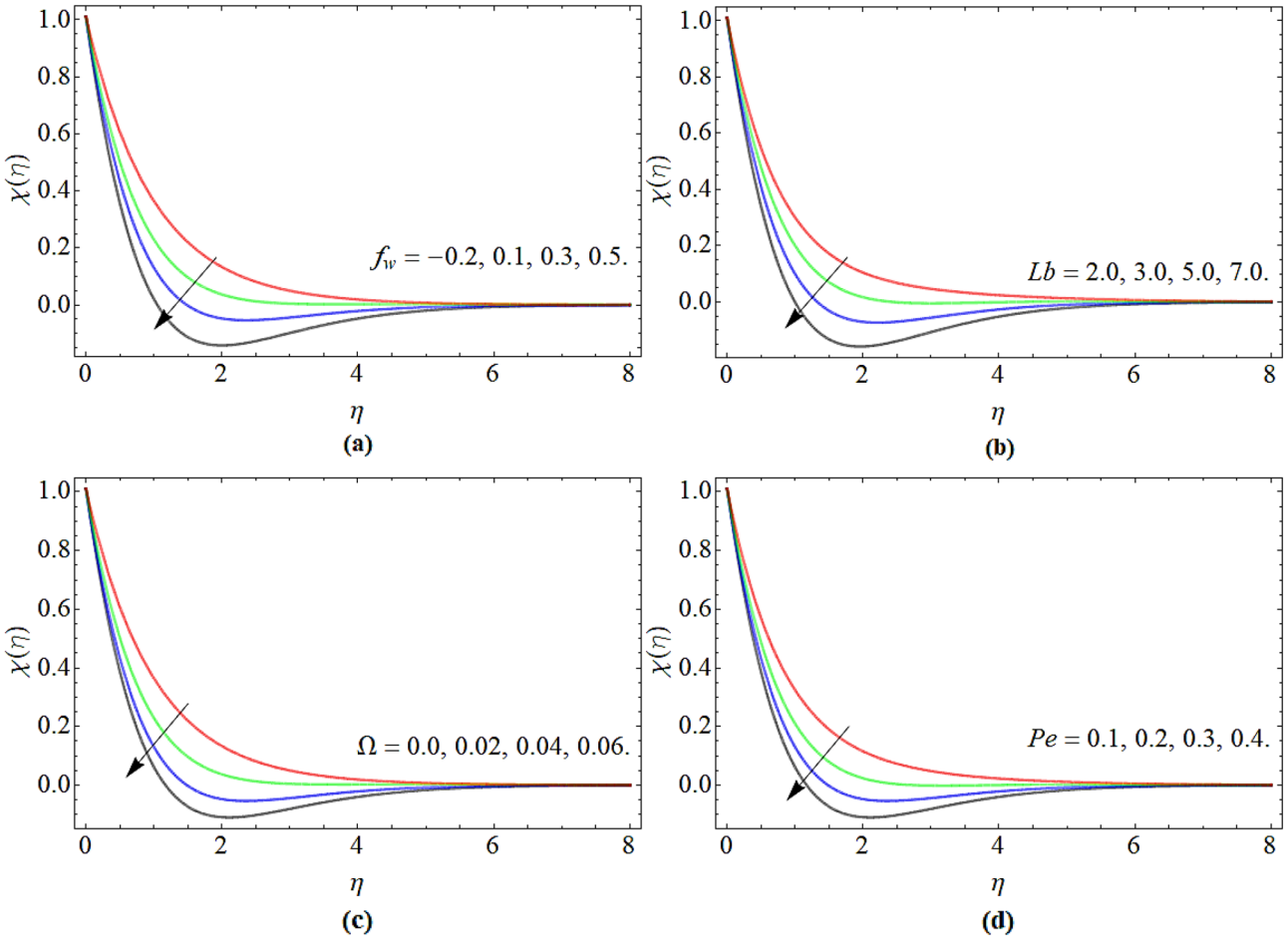

Figure 5. The nature of motile microbe $\chi(\eta)$ profile versus (**a**) suction/injection f_w, (**b**) bio-convection Lewis number Lb, (**c**) microbe concentration variance Ω, (**d**) bioconvection Peclet number Pe respectively.

Approximation order	$f'(0)$	$-g'(0)$
Current result	0.599482	0.600872
Mutuku & Makinde[50]	0.597211	0.609633
Xun et al.[54]	0.510231	0. 615921

Table 1. Comparative assessment of current outcomes with the published work.

Data availability

All data used in this manuscript have been presented within the article.

Received: 18 December 2021; Accepted: 10 February 2022
Published online: 25 February 2022

References

1. Ahmadian, A., Bilal, M., Khan, M. A. & Asjad, M. I. The non-Newtonian maxwell nanofluid flow between two parallel rotating disks under the effects of magnetic field. *Sci. Rep.* **10**(1), 1–14 (2020).
2. Lv, Y. P. *et al.* Numerical approach towards gyrotactic microorganisms hybrid nanoliquid flow with the hall current and magnetic field over a spinning disk. *Sci. Rep.* **11**(1), 1–13 (2021).
3. Li, Y. X. *et al.* Fractional simulation for Darcy-Forchheimer hybrid nanoliquid flow with partial slip over a spinning disk. *Alex. Eng. J.* **60**(5), 4787–4796 (2021).
4. Shuaib, M., Shah, R. A. & Bilal, M. Von-Karman rotating flow in variable magnetic field with variable physical properties. *Adv. Mech. Eng.* **13**(2), 1687814021990463 (2021).
5. Bilal, M. *et al.* Numerical approximation of microorganisms hybrid nanofluid flow induced by a wavy fluctuating spinning disc. *Coatings* **11**(9), 1032 (2021).
6. Tassaddiq, A. *et al.* Heat and mass transfer together with hybrid nanofluid flow over a rotating disk. *AIP Adv.* **10**(5), 055317 (2020).
7. Noghrehabadi, A., Saffarian, M. R., Pourrajab, R. & Ghalambaz, M. Entropy analysis for nanofluid flow over a stretching sheet in the presence of heat generation/absorption and partial slip. *J. Mech. Sci. Technol.* **27**(3), 927–937 (2013).

8. Khan, M. I., Shah, F., Khan, S. U., Ghaffari, A., & Chu, Y. M. Heat and mass transfer analysis for bioconvective flow of Eyring Powell nanofluid over a Riga surface with nonlinear thermal features. *Numer. Methods Partial Differ. Eq.* (2020).
9. Khan, M. I., Qayyum, S., Chu, Y. M., & Kadry, S. Numerical simulation and modeling of entropy generation in Marangoni convective flow of nanofluid with activation energy. *Numer. Methods Partial Differ. Eq.* (2020).
10. Reza-E-Rabbi, S., Ahmmed, S. F., Arifuzzaman, S. M., Sarkar, T. & Khan, M. S. Computational modelling of multiphase fluid flow behaviour over a stretching sheet in the presence of nanoparticles. *Eng. Sci. Technol. Int. J.* **23**(3), 605–617 (2020).
11. Reza-E-Rabbi, S., Arifuzzaman, S. M., Sarkar, T., Khan, M. S. & Ahmmed, S. F. Explicit finite difference analysis of an unsteady MHD flow of a chemically reacting Casson fluid past a stretching sheet with Brownian motion and thermophoresis effects. *J. King Saud Univ. Sci.* **32**(1), 690–701 (2020).
12. Al-Mamun, A. *et al.* Numerical simulation of periodic MHD Casson nanofluid flow through porous stretching sheet. *SN Appl. Sci.* **3**(2), 1–14 (2021).
13. Bhatti, M. M. & Michaelides, E. E. Study of Arrhenius activation energy on the thermo-bioconvection nanofluid flow over a Riga plate. *J. Therm. Anal. Calorim.* **143**(3), 2029–2038 (2021).
14. Zhang, X. H. *et al.* The parametric study of hybrid nanofluid flow with heat transition characteristics over a fluctuating spinning disk. *PLoS ONE* **16**(8), e0254457 (2021).
15. Algehyne, E. A. *et al.* Thermal improvement in pseudo-plastic material using ternary hybrid nanoparticles via non-Fourier's law over porous heated surface. *Energies* **14**(23), 8115 (2021).
16. Khan, N. M., Bacha, H. B., Pan, K. & Saeed, T. Nonlinear Eyring–Powell bioconvective nanofluid flow over a vertical plate with temperature dependent viscosity and surface suction. *Int. Commun. Heat Mass Transf.* **128**, 105602 (2021).
17. Khan, N. M., Ullah, N., Khan, J. Z., Qaiser, D. & Khan, M. R. Analysis of Maxwell bioconvective nanofluids with surface suction and slip conditions in the presence of solar radiations. *J. Phys. Commun.* **5**(11), 115014 (2021).
18. Khan, N. M., Chu, Y. M., Ijaz Khan, M., Kadry, S., & Qayyum, S. (2020). Modeling and dual solutions for magnetized mixed convective stagnation point flow of upper convected Maxwell fluid model with second-order velocity slip. *Math. Methods Appl. Sci.*
19. AlQdah, K. S., Khan, N. M., Bacha, H. B., Chung, J. D. & Shah, N. A. Marangoni convection of dust particles in the boundary layer of maxwell nanofluids with varying surface tension and viscosity. *Coatings* **11**(9), 1072 (2021).
20. Tsurutani, B. T., Gonzalez, W. D., Lakhina, G. S., & Alex, S. (2003). The extreme magnetic storm of 1–2 September 1859. *J. Geophys. Res. Space Phys. 108*(A7).
21. Fraser-Smith, A. C. *et al.* Low-frequency magnetic field measurements near the epicenter of the Ms 7.1 Loma Prieta earthquake. *Geophys. Res. Lett.* **17**(9), 1465–1468 (1990).
22. Mahmoud, E. E., Algehyne, E. A., Alqarni, M. M., Afzal, A., & Ibrahim, M. (2021). Investigating the thermal efficiency and pressure drop of a nanofluid within a micro heat sink with a new circular design used to cool electronic equipment. *Chem. Eng. Commun.* 1–13.
23. Rashidi, S., Esfahani, J. A. & Maskaniyan, M. Applications of magnetohydrodynamics in biological systems—a review on the numerical studies. *J. Magn. Magn. Mater.* **439**, 358–372 (2017).
24. Bilal, M. *et al.* Darcy-forchheimer hybrid nano fluid flow with mixed convection past an inclined cylinder. *CMC Comput. Mater. Contin.* **66**, 2025–2039 (2021).
25. Zhou, S. S., Bilal, M., Khan, M. A. & Muhammad, T. Numerical analysis of thermal radiative Maxwell nanofluid flow over-stretching porous rotating disk. *Micromachines* **12**(5), 540 (2021).
26. Shuaib, M., Bilal, M. & Qaisar, S. Numerical study of hydrodynamic molecular nanoliquid flow with heat and mass transmission between two spinning parallel plates. *Phys. Scr.* **96**(2), 025201 (2020).
27. Goyal, R., Sharma, N. & Bhargava, R. GFEM analysis of MHD nanofluid flow toward a power-law stretching sheet in the presence of thermodiffusive effect along with regression investigation. *Heat Transf.* **50**(1), 234–256 (2021).
28. Ghasemi, S. E. & Hatami, M. Solar radiation effects on MHD stagnation point flow and heat transfer of a nanofluid over a stretching sheet. *Case Stud. Therm. Eng.* **25**, 100898 (2021).
29. Rasool, G., Shafiq, A. & Durur, H. Darcy-Forchheimer relation in Magnetohydrodynamic Jeffrey nanofluid flow over stretching surface. *Discrete Contin. Dyn. Syst. S* **14**(7), 2497 (2021).
30. Mabood, F., Ashwinkumar, G. P. & Sandeep, N. Simultaneous results for unsteady flow of MHD hybrid nanoliquid above a flat/slendering surface. *J. Therm. Anal. Calorim.* **146**(1), 227–239 (2021).
31. Shuaib, M., Bilal, M. & Khan, M. A. An application of fractional derivatives to a thermo-convective viscous fluid with Dufour and Schmidt effects over a rotating disk. *J. Comput. Methods Sci. Eng.* **20**(2), 645–664 (2020).
32. Shuaib, M., Bilal, M., Khan, M. A. & Malebary, S. J. Fractional analysis of viscous fluid flow with heat and mass transfer over a flexible rotating disk. *Comput. Model. Eng. Sci.* **123**(1), 377–400 (2020).
33. Wakif, A., Animasaun, I. L., & Sehaqui, R. (2021). A brief technical note on the onset of convection in a horizontal nanofluid layer of finite depth via Wakif-Galerkin weighted residuals technique (WGWRT). In *Defect and Diffusion Forum* (Vol. 409, pp. 90–94). Trans Tech Publications Ltd.
34. Wakif, A., & Sehaqui, R. (2020). Generalized differential quadrature scrutinization of an advanced MHD stability problem concerned water-based nanofluids with metal/metal oxide nanomaterials: a proper application of the revised two-phase nanofluid model with convective heating and through-flow boundary conditions. *Numer. Methods Partial Differ. Eq.*
35. Ali, B., Shafiq, A., Manan, A., Wakif, A. & Hussain, S. Bioconvection: Significance of mixed convection and mhd on dynamics of Casson nanofluid in the stagnation point of rotating sphere via finite element simulation. *Math. Comput. Simul.* **194**, 254–268 (2022).
36. Dawar, A., Wakif, A., Thumma, T. & Shah, N. A. Towards a new MHD non-homogeneous convective nanofluid flow model for simulating a rotating inclined thin layer of sodium alginate-based Iron oxide exposed to incident solar energy. *Int. Commun. Heat Mass Transf.* **130**, 105800 (2022).
37. Sabu, A. S., Wakif, A., Areekara, S., Mathew, A. & Shah, N. A. Significance of nanoparticles' shape and thermo-hydrodynamic slip constraints on MHD alumina-water nanoliquid flows over a rotating heated disk: The passive control approach. *Int. Commun. Heat Mass Transf.* **129**, 105711 (2021).
38. Kuznetsov, A. V. The onset of nanofluid bioconvection in a suspension containing both nanoparticles and gyrotactic microorganisms. *Int. Commun. Heat Mass Transf.* **37**(10), 1421–1425 (2010).
39. Geng, P. & Kuznetsov, A. V. Effect of small solid particles on the development of bioconvection plumes. *Int. Commun. Heat Mass Transf.* **31**(5), 629–638 (2004).
40. Rana, B. M. J. *et al.* Swimming of microbes in blood flow of nano-bioconvective Williamson fluid. *Therm. Sci. Eng. Progress* **25**, 101018 (2021).
41. Gharami, P. P. Reza-E-Rabbi. 1–16.
42. Kuznetsov, A. V. Non-oscillatory and oscillatory nanofluid bio-thermal convection in a horizontal layer of finite depth. *Eur. J. Mech. B/Fluids* **30**(2), 156–165 (2011).
43. Xu, Y. J., Bilal, M., Al-Mdallal, Q., Khan, M. A. & Muhammad, T. Gyrotactic micro-organism flow of Maxwell nanofluid between two parallel plates. *Sci. Rep.* **11**(1), 1–13 (2021).
44. Waqas, H. *et al.* Falkner-Skan time-dependent bioconvrction flow of cross nanofluid with nonlinear thermal radiation, activation energy and melting process. *Int. Commun. Heat Mass Transf.* **120**, 105028 (2021).

45. Ramzan, M., Gul, H., Chung, J. D., Kadry, S. & Chu, Y. M. Significance of Hall effect and Ion slip in a three-dimensional bioconvective Tangent hyperbolic nanofluid flow subject to Arrhenius activation energy. *Sci. Rep.* **10**(1), 1–15 (2020).
46. Khan, M. I. *et al.* Slip flow of micropolar nanofluid over a porous rotating disk with motile microorganisms, nonlinear thermal radiation and activation energy. *Int. Commun. Heat Mass Transf.* **122**, 105161 (2021).
47. Ramzan, M., Gul, H., Kadry, S. & Chu, Y. M. Role of bioconvection in a three dimensional tangent hyperbolic partially ionized magnetized nanofluid flow with Cattaneo-Christov heat flux and activation energy. *Int. Commun. Heat Mass Transf.* **120**, 104994 (2021).
48. Ashraf, M. *et al.* Computational analysis of the effect of nano particle material motion on mixed convection flow in the presence of heat generation and absorption. *CMcC Comput. Mater. Contin.* **65**(2), 1809–1823 (2020).
49. Olanrewaju, A. M. & Makinde, O. D. On boundary layer stagnation point flow of a nanofluid over a permeable flat surface with Newtonian heating. *Chem. Eng. Commun.* **200**(6), 836–852 (2013).
50. Mutuku, W. N. & Makinde, O. D. Hydromagnetic bioconvection of nanofluid over a permeable vertical plate due to gyrotactic microorganisms. *Comput. Fluids* **95**, 88–97 (2014).
51. Sarkar, A., Das, K. & Kundu, P. K. On the onset of bioconvection in nanofluid containing gyrotactic microorganisms and nanoparticles saturating a non-Darcian porous medium. *J. Mol. Liq.* **223**, 725–733 (2016).
52. Shuaib, M., Shah, R. A. & Bilal, M. Variable thickness flow over a rotating disk under the influence of variable magnetic field: An application to parametric continuation method. *Adv. Mech. Eng.* **12**, 1687814020936385 (2020).
53. Shuaib, M., Shah, R. A., Durrani, I. & Bilal, M. Electrokinetic viscous rotating disk flow of Poisson-Nernst-Planck equation for ion transport. *J. Mol. Liq.* **313**, 113412 (2020).
54. Xun, S., Zhao, J., Zheng, L., Chen, X. & Zhang, X. Flow and heat transfer of Ostwald-de Waele fluid over a variable thickness rotating disk with index decreasing. *Int. J. Heat Mass Transf.* **103**, 1214–1224 (2016).

Acknowledgements

The authors acknowledge the financial support provided by the Center of Excellence in Theoretical and Computational Science (TaCS-CoE), KMUTT. Moreover, this research project is supported by Thailand Science Research and Innovation (TSRI) Basic Research Fund: Fiscal year 2022 (FF65).

Author contributions

All authors are equally contributed.

Competing interests

The authors declare no competing interests.

Additional information

Correspondence and requests for materials should be addressed to P.K.

Reprints and permissions information is available at www.nature.com/reprints.

Publisher's note Springer Nature remains neutral with regard to jurisdictional claims in published maps and institutional affiliations.